J Physiol (2003), **548.1**, *pp.* 21–29

DOI: 10.1113/jphysiol.2002.034918
www.jphysiol.org

Journal of Physiology

PSD-95 regulates NMDA receptors in developing cerebellar granule neurons of the rat

Gabriele Losi*, Kate Prybylowski*†, Zhanyan Fu*‡, Jianhong Luo*‡, Robert J. Wenthold† and Stefano Vicini*

**Department of Physiology and Biophysics, Georgetown University, Washington DC, †Laboratory of Neurochemistry, NIDCD, NIH, Bethesda, MD, USA and ‡Laboratory of Neurobiology, Zhejiang University, Hangzhou, China*

We transfected a green fluorescent protein-tagged PSD-95 (PSD-95gfp) into cultured rat cerebellar granule cells (CGCs) to investigate the role of PSD-95 in excitatory synapse maturation. Cells were grown in low potassium to favour functional synapse formation *in vitro*. Transfected cells displayed clear clusters of PSD-95gfp, often at the extremities of the short dendritic trees. We recorded NMDA and AMPA miniature excitatory postsynaptic currents (NMDA- and AMPA-mESPCs) in the presence of TTX and bicuculline. At days *in vitro* (DIV) 7–8 PSD-95gfp-transfected cells had NMDA-mEPSCs with faster decay and smaller amplitudes than matching controls. In contrast, AMPA-mEPSC frequencies and amplitudes were increased. Whole-cell current density and ifenprodil sensitivity were reduced in PSD-95gfp cells, indicating a reduction of NR2B subunits containing NMDA receptors. No changes were observed compared to control when cells were transfected with cDNA for PSD-95gfp with palmitoylation site mutations that prevent targeting to the synapse. Overexpression of the NMDA receptor NR2A subunit, but not the NR2B subunit, prevented NMDA-mEPSC amplitude reduction when cotransfected with PSD-95gfp. PSD-95gfp overexpression produced faster NMDA-mEPSC decay when transfected alone or with either NR2 subunit. Surface staining of the epitope-tagged NR2 subunits revealed that colocalization with PSD-95gfp was higher for flag-tagged NR2A subunit clusters than for flag-tagged NR2B subunit clusters. These data suggest that PSD-95 overexpression in CGCs favours synaptic maturation by allowing synaptic insertion of NR2A and depressing expression of NR2B subunits.

(Received 24 October 2002; accepted after revision 15 January 2003; first published online 7 February 2003)
Corresponding author S. Vicini: Department of Physiology and Biophysics, Georgetown University, Box 571460, Basic Science Building Room 225, Washington DC 20057-1460, USA. Email: svicin01@georgetown.edu

In rodent cerebellar granule cells (CGCs), NMDA receptor NR2B subunit protein expression levels decrease during the second postnatal week whilst NR2A subunit expression increases (Cull-Candy *et al.* 2001 for review). The developmental changes of NR2 subunit expression and the distinct kinetics of NR1/NR2A and NR1/NR2B receptors (Monyer *et al.* 1994; Vicini *et al.* 1998) underlie the developmental change of NMDA-EPSC kinetics (Rumbaugh & Vicini, 1999; Cathala *et al.* 2000).

In postsynaptic densities (PSDs) the cytosolic C-terminal tails of NMDA receptors associate with distinct PSD-95/discs large/zona occludens-1 (PDZ) domain-containing synaptic scaffolding proteins (Kornau *et al.* 1997; Ziff, 1997; Garner *et al.* 2000). The C-terminals of NR2 subunits bind to PDZ domains of the membrane-associated guanylate kinases (MAGUKs) superfamily (Kornau *et al.* 1997; Garner *et al.* 2000) of which PSD-95/synapse-associated protein-90 (termed PSD-95 in this text) is the major component. Yet in hippocampal neurons, PSD-95 overexpression increases AMPA synaptic response and AMPA receptor expression at synapses but does not affect NMDA receptor expression or response (El-Husseini *et al.* 2000; Schnell *et al.* 2002).

The regulation of AMPA receptors (AMPARs) was not seen with overexpression of a construct with mutation of N-terminal cysteines into serines in PSD-95, preventing the palmitoylation of the protein (PSD-95gfpC35S, Craven *et al.* 1999). It has recently been shown that green fluorescent protein-tagged PSD-95 (PSD-95gfp) specifically increases synaptic insertion of AMPARs in the hippocampal slice due to interactions between PSD-95 and stargazin, without changing the number of surface AMPARs (Schnell *et al.* 2002).

In situ hybridization studies indicate that the increase in PSD-95 mRNA occurs later in the cerebellum than in the hippocampus (Fukaya *et al.* 1999; Fukaya & Watanabe, 2000), therefore overexpression of PSD-95gfp in cerebellar granule cells may be an interesting model system. In addition, the small size of cerebellar granule cells makes it possible to record NMDA-mEPSCs with good resolution

and ideal voltage-clamp conditions (Silver *et al.* 1992), providing a unique reliable model in which to study NMDA receptors at individual synapses (Clark *et al.* 1997; Prybylowski *et al.* 2002). For these reasons we investigated the effect of PSD-95gfp (Craven *et al.* 1999) overexpression on NMDA-mEPSCs recorded from CGCs in primary culture under conditions that favour functional synaptic transmission (Virginio *et al.* 1995; Mellor *et al.* 1998; Chen *et al.* 2000; Prybylowski *et al.* 2002). We also studied the effect of PSD-95 transfection on recombinant NMDA receptors in HEK 293 cells. Lastly, taking advantage of N-terminal tagging of NR2A and NR2B subunits with flag epitope, we investigated the colocalization of these subunits with PSD-95gfp puncta.

METHODS

Cerebellar granule cell culture

Primary cultures of rat cerebellar granule neurons were prepared from postnatal day 7 (P7) Sprague-Dawley rat cerebella. Rat pups were killed as required by the guidelines of the Georgetown University Animal Care and Use Committee by decapitation and cerebellar cells were dissociated as described in Gallo *et al.* 1987. Cells were dispersed with trypsin (0.25 mg ml^{-1}; Sigma, St Louis, MO, USA) and plated at a density of 1.1×10^6 cells ml^{-1} on glass coverslips coated with poly-L-lysine (10 μg ml^{-1}; Sigma) in 35 mm Nunc dishes. Cells were cultured in basal Eagle's medium supplemented with 10 % bovine calf serum, 2 mM glutamine and 100 μg ml^{-1} gentamicin (all from Invitrogen Corporation, Carlsbad, CA, USA) and maintained at 37 °C in 6 % CO_2. The final concentration of KCl in the culture medium was adjusted to 25 mM (high K^+). To achieve functional synapse formation, at DIV 4 medium was replaced with low (5 mM) K^+ medium (MEM supplemented with 5 mg ml^{-1} glucose, 0.1 mg ml^{-1} transferrin, 0.025 mg ml^{-1} insulin, 2 mM glutamine, 20 μg ml^{-1} gentamicin (Invitrogen) and cytosine arabinofuranoside (10 μM; Sigma) as previously described (Chen *et al.* 2000; Prybylowski *et al.* 2002). Recordings were made from DIV 6–12 neurons in culture.

DNA constructs and CGC transfection

The rat NR2B-flag (NR2B subunit tagged at the N-terminal with flag epitope, a gift of Dr Anne Stephenson, School of Pharmacy, University College, London) has been previously described (Hawkins *et al.* 1999; Prybylowski *et al.* 2002). The human NR2A-flag (NR2A subunit tagged at the N-terminal with flag epitope, a gift of Dr Paul Whiting, Merck Sharp and Dohme, Harlow, UK) has been described previously (McIlhinney *et al.* 1998). Although flag-tagged NR2 subunits were derived from different species, NMDA receptor (NMDAR) subunits in rat and human have over 95 % homology. PSD-95gfp and PSD-95gfpC35S were generous gifts of Dr David Bredt (University of California, San Francisco, CA, USA) and are described in Craven *et al.* 1999. The NR1–1a construct was described in Vicini *et al.* 1998.

CGC transfection

Primary cultures of rat CGCs were transfected using a modification of the calcium phosphate precipitation technique as reported in Prybylowski *et al.* 2002. Briefly, cultured neurons at DIV 5 on a glass coverslip were transferred to a well in a 4-well plate with 500 μl transfection medium, a MEM medium (Catalogue no. 12370-037, Invitrogen) with pH adjusted to 7.85 by 5 M NaOH. Then 30 μl DNA/Ca^{2+} mixture containing 3 μg cDNA was added and incubated for 30 min at room temperature. After two washes with the transfection medium, it was replaced with original culture medium and neurons were maintained at 37 °C in 5 % CO_2. EGFP plasmid (Clontech, Palo Alto, CA, USA) was also transfected to allow visualization of successfully transfected cells (except for experiments with PSD-95gfp and PSD-95gfpC35S constructs). Each coverslip was transfected with 0.3 μg EGFP plasmid, and 1 μg of NMDA subunit and PSD-95 construct. If cells were transfected with only one NMDA subunit or PSD-95 construct, 1 μg of plasmid DNA for NR2A in pBluescript (containing a bacterial promoter) was used to control for equal amounts of DNA for each transfection. To assess transfection efficacy, cells were counted on more than 20 coverslips in at least eight distinct transfections. HEK 293 cells were transfected with NR2A-flag or NR2B-flag and NR1–1a cDNA as described in Vicini *et al.* 1998.

Solutions and drugs

The recording chamber was continuously perfused at 5 ml min^{-1} with an extracellular medium composed, for cultured neurons, of (mM): NaCl (145), KCl (5), $MgCl_2$ (1), $CaCl_2$ (1), Hepes (5), glucose (5), sucrose (25), phenol red (0.25 mg l^{-1}) and D-serine (5 μM) (all from Sigma) adjusted to pH 7.4 with NaOH. All experiments were performed at room temperature (24–26 °C). CGCs were voltage clamped at −60 mV and a recording solution was used containing (mM): potassium gluconate (145), Hepes (10), ATP-Mg (5), GTP-Na (0.2) and BAPTA (10), adjusted to pH 7.2 with KOH. Electrodes were pulled in two stages on a vertical pipette puller from borosilicate glass capillaries (Wiretrol II, Drummond, Broomall, PA, USA). Typical pipette resistance was 5–7 MΩ. NMDAR-mediated responses were pharmacologically isolated by bicuculline methiodide (BMI, 50 μM; Sigma) and 2,3-dihydro-6-nitro-7-sulfamoyl-benzo(f)quinoxaline (NBQX, 5 μM; Tocris). Ifenprodil (10 μM; Sigma), an NR2B selective blocker (Williams 1993), was pre-perfused and co-applied with NMDA. AMPA-mEPSCs were recorded at −60 mV in the presence of 1 μM tetrodotoxin (TTX; Sigma) and 50 μM BMI. NMDA-mEPSCs were recorded at −60 mV in Mg^{2+}-free solution in the presence of 1 μM TTX, 5 μM NBQX and 50 μM BMI. Drugs were superfused through parallel inputs to the perfusion chamber or locally perfused by means of a Y tube (Murase *et al.* 1989).

Electrophysiology

Whole-cell recordings were performed with a patch-clamp amplifier (Axopatch 200, Axon Instrument, Union City, CA, USA). CGCs were voltage clamped at −60 mV and access resistance was monitored throughout the recordings. Capacitance was assessed from the transient current in response to a 10 mV hyperpolarizing pulse. Single channel currents were identified in recordings of NMDA-mEPSCs. Single channel current amplitude estimates from the tails of synaptic currents were analysed using the Fetchan and Pstat routines of the pCLAMP 6.03 software suite. Rare openings at subconductance levels were excluded from the amplitude analysis. Small lifted HEK cells and nucleated patches pulled from transfected and control CGCs were placed in the flow of the piezo-driven (P-245.30 Stacked Translator, Physik Instrumente, Waldbronn, Germany) double-barrel pipette as in Vicini *et al.* 1998. Control solution for double-barrel application contained 0.2 mM $CaCl_2$ (to minimize rundown of the response over repeated agonist applications), 5 μM NBQX (to block AMPA responses) and 20 μM D-serine in Mg^{2+}-free solution. Brief (4 ms) solution exchanges were then made into a solution which also contained 1 mM glutamate.

Data collection and analysis

Currents were filtered at 1 kHz with an 8-pole low-pass Bessel filter (Frequency Devices, Haverhill, MA, USA), digitized at 5–10 kHz using an IBM-compatible microcomputer equipped with a Digidata 1200 data acquisition board and pCLAMP 8 software (both from Axon Instruments). Off-line data analysis, curve fitting and figure preparation were performed with Clampfit 8 (Axon Instruments) and Origin 4.1 (MicroCal Inc., Northampton, MA, USA) software. Miniature synaptic currents were identified using a semi-automated mini detection software (Minianalysis, Synaptosoft, Decatur, GA, USA) with threshold criteria of 7.5 pA, threefold greater than the RMS noise level of 2.5 pA and approximately equivalent to two overlapping channel openings. NMDA-mEPSC averages were of at least 30 events in each cell studied.

Fitting of the decay phase of currents recorded from CGCs and HEK 293 cells was performed using a simplex algorithm for least squares exponential fitting routines. Decay times of averaged currents derived from fitting to double exponential equations of the form:

$$I(t) = I_f \exp(-t/\tau_f) + I_s \exp(-t/\tau_s),$$

where I_f and I_s are the amplitudes of the fast and slow decay components, and τ_f and τ_s are their respective decay time constants used to fit the data. To compare decay time between different subunit combinations we used a weighted mean decay time constant:

$$\tau_w = (I_f/(I_f + I_s))\tau_f + (I_s/(I_f + I_s))\tau_s.$$

Data values are expressed as means ± S.E.M. unless otherwise indicated. *P* values represent the analysis of variance (ANOVA) for multiple comparisons.

Immunocytochemistry

All incubations for staining experiments were carried out at room temperature. To determine PSD-95 overexpression, cultured CGCs were fixed in 4 % paraformaldehyde, 4 % sucrose in phosphate-buffered saline (PBS) for 5 min and then incubated in 0.025 % Triton X-100 for 3 min. Cells were preincubated in 10 % BSA (Sigma) for 1 h and then incubated with primary antibodies in PBS containing 3 % BSA for 1 h. Monoclonal antibody against PSD-95 (clone 6G9–1C9; Affinity Bioreagents, Golden, CO, USA; interacts with other members of the PSD/SAP family) was used at 1:2000. After washing with PBS several times, cells were incubated with secondary antibodies for 1 h. Both indocarbocyanine (Cy3)-conjugated goat anti-mouse and anti-rabbit IgG antibodies (Jackson ImmunoResearch laboratories, West Grove, PA, USA) were used at 1:2000. Coverslips were observed unmounted.

We performed surface staining of live cultured CGCs transfected with PSD-95gfp plus flag-tagged NR2A or NR2B subunits. CGCs were incubated with monoclonal antibodies against flag (Sigma) at 1:100 in extracellular medium for 6 min at room temperature. After three PBS washes, cells were incubated with indocarbocyanine (Cy3)-conjugated anti-mouse antibody at 1:400 for 6 min. Cultures were then fixed with paraformaldehyde and imaged. Spectral characteristics of the excitation–emission filters used were 490/530 nm for GFP and 545/610 nm for Cy3, respectively. Neurons were imaged on a Nikon EN600 microscope equipped with a 60 ×, 1.0 NA objective with a 12-bit cooled CCD digital camera, (Hamamatsu Orca-100) with 1392 × 1040 pixel array. Images were captured and pseudocoloured for presentation using MetaMorph imaging software (Universal Imaging Corporation, Downingtown, PA, USA) and Adobe Photoshop 6.0. Antibody-positive receptor clusters were defined as clusters of fluorescence that were at least twice the background fluorescence of the image. Colocalization of PSD-95gfp and flag-positive puncta was defined as having at least 50 % overlapping pixels. Surface staining for NR1–1a-gfp clusters was carried out in a similar manner, using 1:400 dilution of anti-gfp primary antibody (Chemicon, Temecula, CA, USA) and 1:400 Cy3-conjugated anti-rabbit antibody. All immunocytochemical analyses were performed blind.

RESULTS

We transfected a green fluorescent protein-tagged PSD-95 (PSD-95gfp) into rat cerebellar granule cells grown in primary culture in a 5 mM K^+ medium that favours functional synaptic transmission. As illustrated in Fig. 1 transfected cells were easily recognized by bright green fluorescent clusters and a low level of diffuse fluorescence. The transfection efficiency was highly variable, being typically less than 1 %. In some cells, (~35 %) clear clusters of PSD-95gfp were located at the extremities of the short dendritic trees, a location suggesting the formation in culture of synaptic structures reminiscent of the glomeruli observed

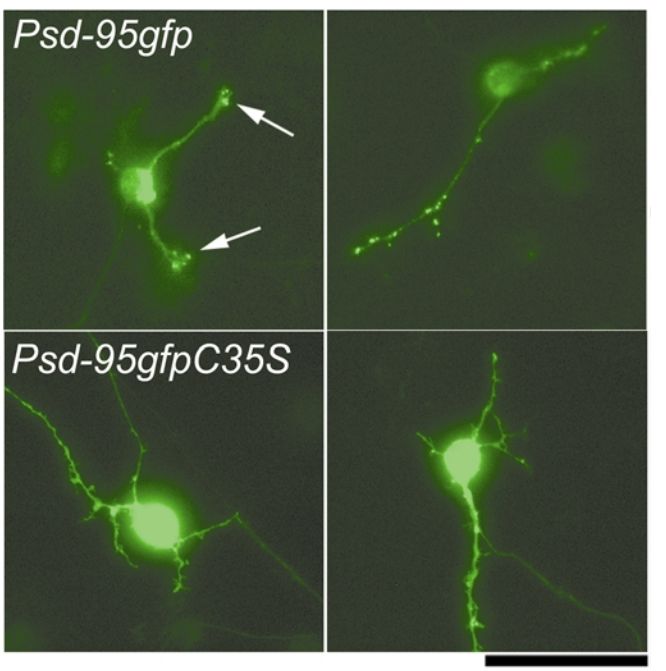

Figure 1. Transfection of cerebellar granule cells (CGCs) with cDNAs for wild-type and mutant green fluorescent protein-tagged PSD-95 (PSD-95gfp)

CGCs were transfected at DIV 5 with cDNAs for PSD-95gfp (top panels). Successfully transfected cells were characterized by green fluorescent clusters and a low level of diffuse fluorescence. In many cells, clusters of PSD-95gfp were located at the extremities of the short dendritic trees (arrows) in positions reminiscent of the glomeruli observed *in vivo*. Transfection of PSD-95gfpC35S led to the expression of diffuse GFP fluorescence (bottom panels). Calibration bar = 18 μm.

in vivo (Palay & Chan-Palay, 1974; Hamori & Somogyi, 1983). It has to be noted, however, that these synapses are quite distinct from those found *in vivo*, as the granule cell cultures lack mossy fibre inputs. Transfection of a PSD-95 construct with the N-terminal palmitoylated cysteines mutated to serines (C35S) so that it does not target the synapse (PSD-95gfpC35S, Craven *et al.* 1999) led to the expression of diffuse GFP fluorescence (Fig. 1). In parallel experiments we used an antibody against MAGUKs to compare the expression of transfected PSD-95gfp with that of the endogenous protein. As reported in hippocampal neurons (Craven *et al.* 1999), exogenous PSD-95gfp was targeted in a manner indistinguishable from endogenous PSD-95 although at higher expression levels (not shown).

PSD-95gfp overexpression leads to synaptic maturation

Using the patch-clamp technique in the whole-cell configuration, we recorded mEPSCs from CGCs in the presence of TTX and bicuculline. AMPA currents were recorded in the presence of 1 mM Mg^{2+}, while the removal of Mg^{2+} in presence of NBQX (5 μM) allowed us to isolate NMDA-mEPSCs. At DIV 7–8 (48–72 h after transfection) PSD-95gfp-transfected cells showed AMPA-mEPSCs with higher frequency of occurrence and higher amplitudes than matching controls (Fig. 2) as previously reported for hippocampal neurons (El-Husseini *et al.* 2000). In addition NMDA-mEPSCs were significantly faster and smaller than matching controls. Figure 2 shows the average values of the weighted time constant of decay (τ_w) and peak amplitudes for the 29 cells studied in six distinct cultures. The frequency ratio of NMDA- *vs.* AMPA-mEPSCs was significantly lower in transfected cells than controls (0.67 ± 0.2 *vs.* 2.9 ± 0.6 Hz, respectively) due to the significant increase of AMPA-mEPSC frequency (Fig. 2). In six granule cells from one culture that we were able to maintain until DIV 12, NMDA-mEPSCs were significantly faster than in neurons at DIV 7 (τ_w: 55 ± 5 and 108 ± 6 ms, respectively). Overexpression of PSD-95gfpC35S did not have any effect on AMPA-mEPSCs (as shown in El-Husseini *et al.* 2000) or NMDA-mEPSC amplitude and kinetics (Fig. 2*B*).

These data suggested that either PSD-95gfp at excitatory synapses in transfected cells directly altered NMDA channel properties such as deactivation kinetics and conductance, or that it altered the relative proportion of NMDA receptor subtypes endowed with distinct deactivation

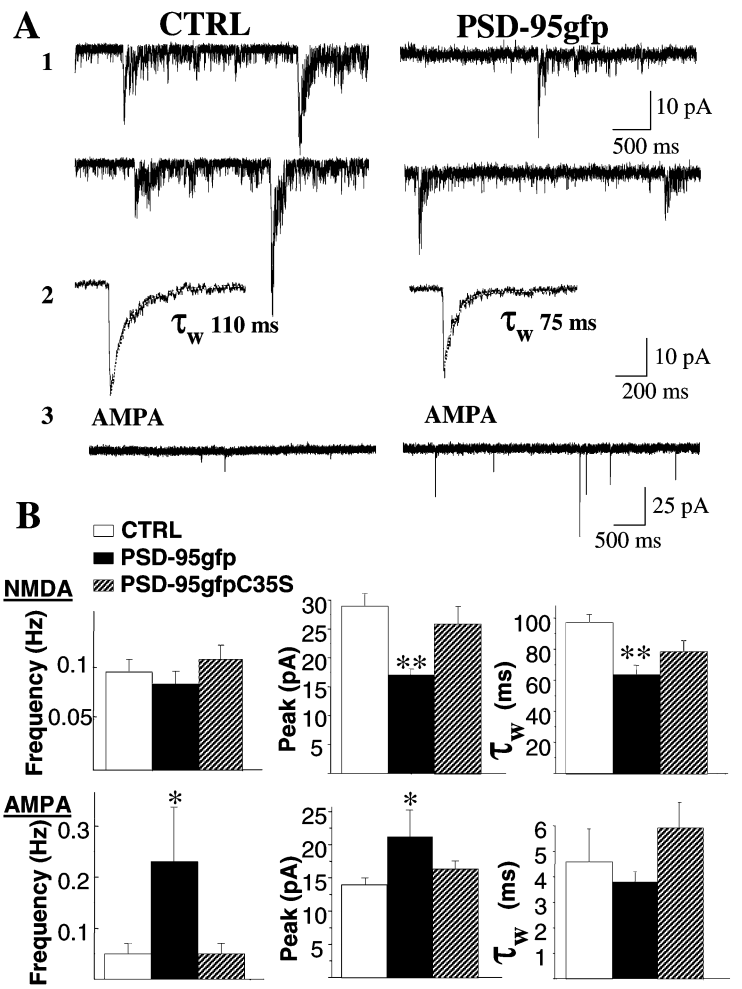

Figure 2. Distinct effects of PSD-95gfp overexpression on miniature EPSCs (mEPSCs) in CGCs in culture

A, representative traces from CGC controls or CGCs transfected with cDNA for PSD-95gfp. *A*1, NMDA-mEPSCs were recorded with exracellular medium containing TTX, BMI and NBQX in the absence of Mg^{2+}. *A*2, averaged NMDA-mEPSCs with superimposed double exponential fitting of the decay phase and indication of resulting weighted time constant (τ_w). *A*3, AMPA-mEPSCs recorded in TTX, BMI and Mg^{2+}. *B*, summaries of frequency, peak amplitude and τ_w of NMDA- (upper panels) or AMPA-mEPSCs (lower panels) recorded from non-transfected CGCs or CGCs transfected with PSD-95gfp or the palmitoylation site mutant PSD-95gfpC35S. Means ± S.E.M., $n > 15$; * $P < 0.05$, ** $P < 0.01$ ANOVA.

kinetics. We therefore investigated the deactivation of responses to brief pulses of glutamate in HEK 293 cells transfected with PSD-95gfp and NR1-1a/NR2A-flag or NR1-1a/NR2B-flag cDNAs. As shown in Fig. 3, PSD-95gfp cotransfection failed to induce significant changes in deactivation kinetics. In contrast, PSD-95gfp transfection shortened the duration of currents elicited by brief pulses of glutamate to nucleated patches excised from granule cells (data not shown). In many cells the high input resistance and low background noise allowed assessment of single channel conductance and open time in the tails of synaptic responses (Silver *et al.* 1992; Clark *et al.* 1997; Prybylowski *et al.* 2002). Single channel conductance and mean open time in eight PSD-95gfp-transfected CGCs (57 ± 1.9 pS; 3.1 ± 0.3 ms) were not significantly different from those in seven control cells (56 ± 2.1 pS; 3.4 ± 0.3 ms).

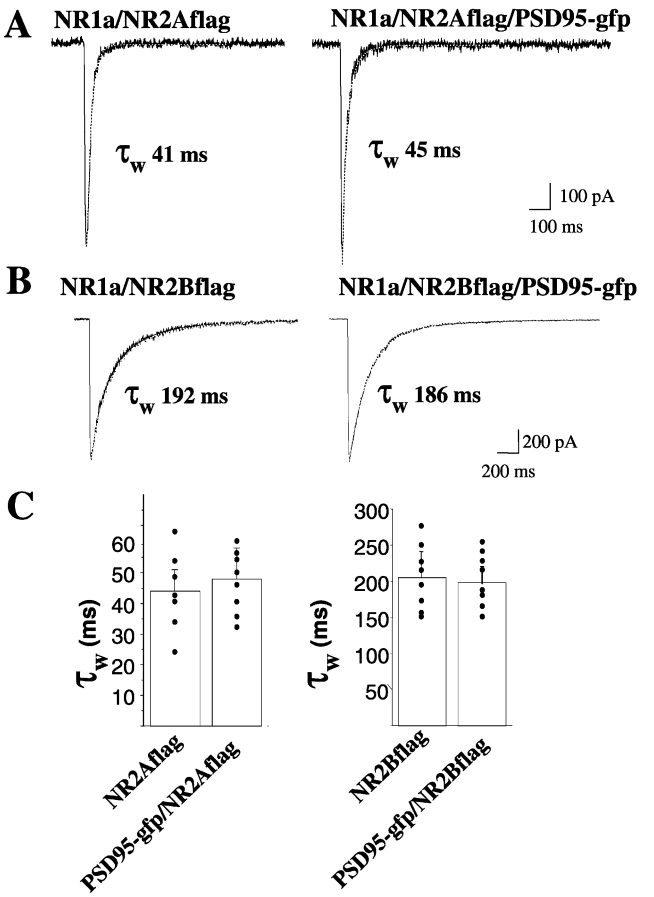

Figure 3. Effect of PSD-95gfp expression on NMDA currents in transfected HEK 293 cells

Responses to brief (4 ms) pulses of 1 mM glutamate/20 μM D-serine elicited in HEK 293 cells transfected with NR1a/NR2A-flag or NR1a/NR2B-flag with or without PSD-95gfp cDNAs. *A* and *B*, average of currents elicited by at least 10 repeated applications with superimposed double exponential fitting and indication of resulting τ_w. *C*, summary of decay time constants for the different transfections.

Whole-cell currents produced by local application of saturating NMDA (200 μM) to CGCs allow an estimate of the total number of receptors (Prybylowski *et al.* 2002). Using this approach we investigated the current density (whole-cell current peak normalized by the cell capacitance) and sensitivity of NMDA application to PSD-95gfp-transfected CGCs to ifenprodil, a selective NR1/NR2B receptor blocker (Williams, 1993). As illustrated in Fig. 4*A* and *B*, NMDA currents were halved in PSD-95gfp-transfected neurons and displayed significantly less blockade by ifenprodil. Figure 4*B* shows the summary percentage reduction induced by ifenprodil of the integral of the NMDA-induced current normalized to the capacitance. Ifenprodil effects were not seen in PSD-95C35S-transfected CGCs (Fig. 4*B*).

Taken together our results suggested that PSD-95gfp was altering the relative proportion of NR1/NR2A and NR1/NR2B NMDA receptor subtypes. Thus we transfected the combination PSD-95gfp/NR2A-flag and PSD-95gfp/NR2B-flag subunits to assess their combined effect on NMDA-

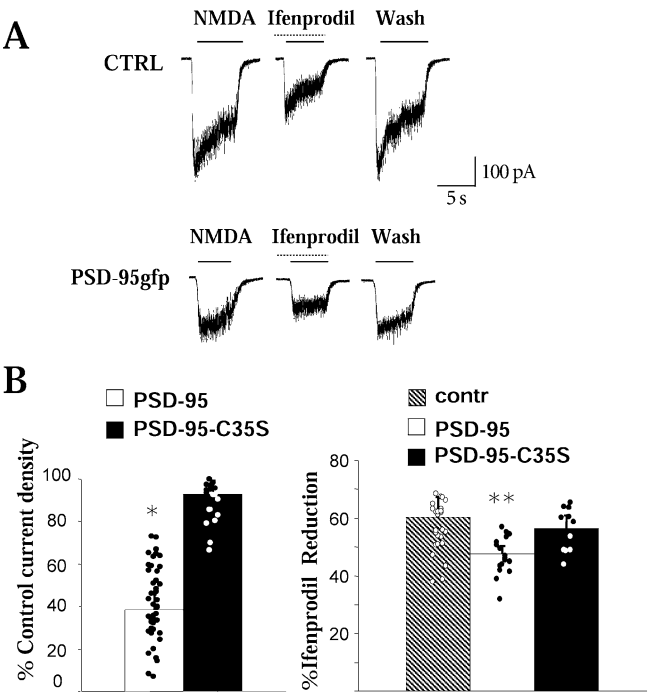

Figure 4. NMDA whole-cell currents and ifenprodil sensitivity in PSD-95gfp-transfected CGCs

A, representative traces showing whole-cell current produced by local application to CGCs of 200 μM NMDA with or without coapplication of 10 μM ifenprodil. In PSD-95gfp-transfected neurons, ifenprodil-induced reduction was weaker. *B*, summary of current densities (left) recorded from CGCs transfected with PSD-95gfp or PSD-95gfpC35S. Shown on the right is the summary percentage reduction by ifenprodil of the integral of the NMDA-induced current normalized to the capacitance. $n > 15$; * $P < 0.05$, ** $P < 0.01$ ANOVA.

mEPSCs as opposed to transfection of either NR2A-flag or NR2B-flag alone. As shown in Prybylowski *et al.* (2002) transfection with either NR2 subunit approximately doubled current density. The current density upon transfection of PSD-95gfp was significantly decreased in NR2B-flag cotransfected cells (68 ± 6 %, $n = 13$) but not in those cotransfected with NR2A-flag (90 ± 9 %, $n = 12$). Similarly, the averaged NMDA-mEPSC amplitude was significantly decreased in PSD-95gfp transfected cells upon cotransfection with NR2B-flag but not with NR2A-flag (Fig. 5). Cotransfection of PSD-95gfp with either NR2A-flag or NR2B-flag subunits accelerated NMDA-mEPSC decay kinetics when compared to the respective flag-tagged NR2 subunits alone (Fig. 5*B*). These results suggest that PSD-95gfp overexpression facilitates synaptic maturation by increasing AMPA receptors, opposing expression of NR2B subunits, and favouring the entry of NR2A subunits at excitatory synapses.

To further support our electrophysiological results we took advantage of the N-terminal location of the flag tag on NMDA receptor subunits to perform live surface staining in cells transfected with PSD-95gfp together with NR2A-flag and NR2B-flag cDNAs. As shown in Fig. 6, NR2A-flag subunit clusters colocalized better with PSD-95gfp puncta than NR2B-flag subunit clusters. In addition the fluorescence intensity of flag-tagged subunit clusters was significantly higher when colocalized with PSD-95 puncta (as compared to non-colocalized clusters) in NR2A-flag but not in NR2B-flag transfected cells (Fig. 6B). Flag surface clusters were lower in density and fluorescence intensity in PSD-95gfp/NR2B-flag transfected CGCs than in those transfected with NR2B-flag alone (not shown).

As previously described (Prybylowski *et al.* 2002), we used the extracellular gfp epitope of NR1–1a-gfp to stain for surface NMDARs in transfected CGCs, as the NR1–1a

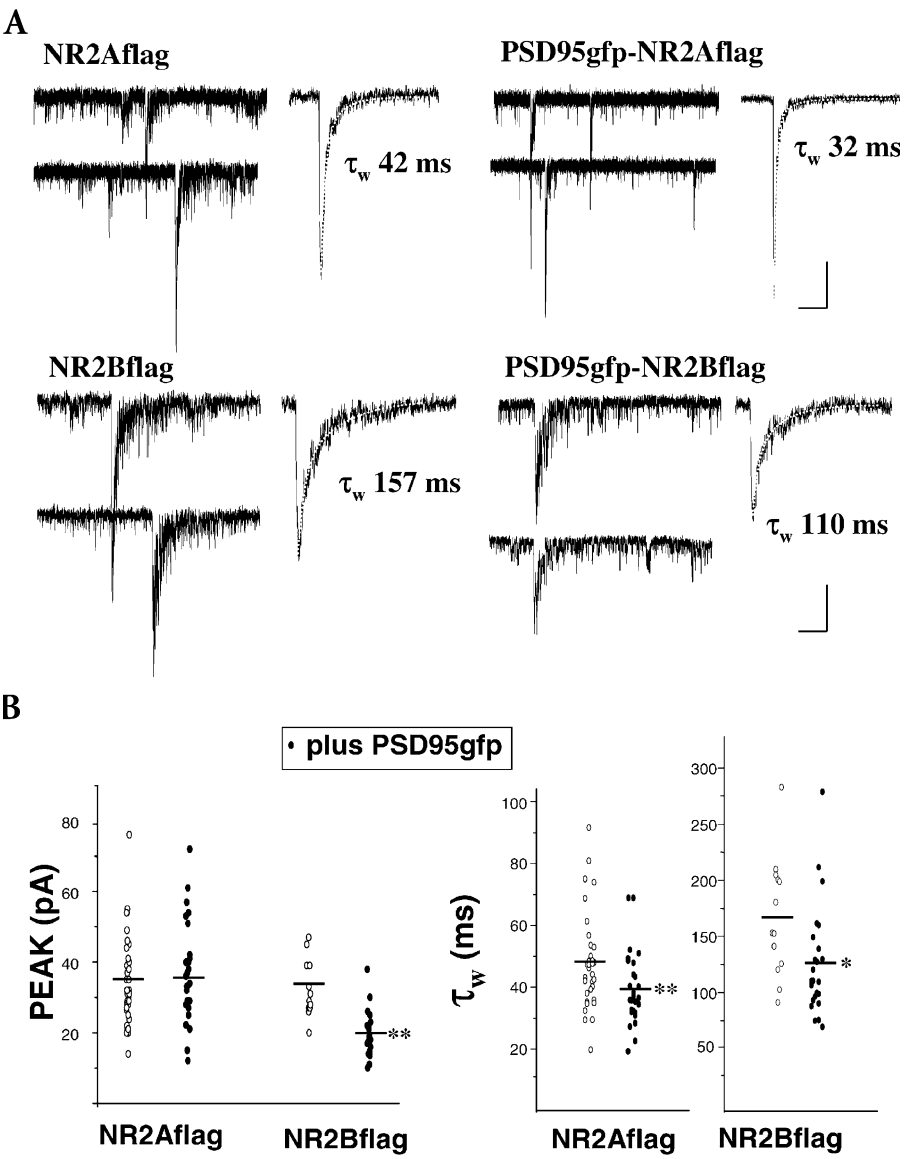

Figure 5. Distinct effects of PSD-95gfp overexpression on NMDA-mEPSCs in NR2A-flag and NR2B-flag transfected CGCs

A, comparison of representative traces from CGCs transfected with cDNAs for NR2A-flag *vs.* NR2A-flag/PSD-95gfp (upper traces) and NR2B-flag *vs.* NR2B-flag/PSD-95gfp (lower traces) recorded in similar conditions to Fig. 2. Shown on right side of each trace panel are NMDA-mEPSC averages with superimposed double exponential fitting and indication of resulting decay time weighted time constant (τ_w). Calibration bars are 10 pA and 500 ms (200 ms for averages). *B*, summary of peak amplitude and τ_w of NMDA-mEPSCs recorded from CGCs transfected with NR2A-flag *vs.* NR2A-flag/PSD-95gfp and NR2B-flag *vs.* NR2B-flag/PSD-95gfp. NMDA-mEPSCs were significantly smaller in cells cotransfected with NR2B-flag/PSD-95gfp than those with NR2A-flag/PSD-95gfp. Both cotransfections shortened the duration of NMDA-mEPSCs. $n > 15$; * $P < 0.05$, ** $P < 0.01$ ANOVA.

splice variant only reaches the surface when assembled with NR2 subunits. Gfp-positive puncta were counted in cells cotransfected with NR1–1a-gfp and either PSD-95gfp or PSD-95gfpC35S. The number of clusters per 10 μm of dendritic length was 9.2 ± 1.3 (n = 10 regions of interest in eight cells in three experiments) for PSD-95gfpC35S-transfected cells and 2.1 ± 0.5 (n = 11 in seven cells) for PSD-95gfp-transfected cells, which was a significant decrease ($P < 0.001$). These data, together with the reduction in current density of NMDA response, confirm that overexpression of PSD-95gfp decreases surface NMDAR expression in CGCs.

DISCUSSION

We report the effect of overexpression of PSD-95, a member of the membrane-associated guanylate kinases superfamily and a major component of the postsynaptic density (Kornau *et al.* 1997; Kennedy, 1998; Garner *et al.* 2000). Our results taken globally suggest that in cerebellar granule neurons, PSD-95 facilitates excitatory synapse maturation by increasing AMPA receptors, opposing expression of NR2B subunits and favouring the entry of NR2A subunits. Indeed *in vivo*, the developmental switch from NR2B to NR2A subunit expression is more dramatic in CGCs as compared to other brain regions (as seen by the decreased duration of NMDA-EPSCs and sensitivity to NR2B specific blockers; Rumbaugh & Vicini, 1999; Cathala *et al.* 2000).

In CGCs in both culture and slices, we recently reported the occurrence of silent synapses, endowed with NMDA receptor only (Losi *et al.* 2002). Our data show that PSD-95 overexpression increases AMPA-mEPSC frequency and amplitude in CGCs in a similar way to that reported in hippocampal neurons (El-Husseini *et al.* 2000; Schnell *et al.* 2002). The decrease of NMDA-/AMPA-mEPSC frequency ratio in PSD-95-transfected CGCs suggests that PSD-95 decreases the occurrence of silent synapses. In contrast to that reported for hippocampal neurons (Schnell *et al.* 2002), PSD-95 overexpression affects NMDA receptors in CGCs. In PSD-95gfp-transfected CGCs, there was a decrease in NMDA-mEPSC amplitude and decay time constant without an effect on NMDA single channel current and open time. However, cotransfection of PSD-95gfp together with NR1–1a/NR2A or NR1–1a/NR2B cDNAs did not alter the deactivation kinetics of glutamate responses in heterologous cells. This suggests that changes in NMDA-mEPSCs with PSD-95gfp transfection are due to an alteration of synaptic NMDA receptor subtypes rather than a direct effect on channel properties, although an indirect effect of PSD-95 on a neuron-specific intermediate protein cannot be excluded. The effects of PSD-95 overexpression on NMDA-mEPSC size and kinetics are paralleled by a reduction in whole-cell current density and ifenprodil sensitivity. A PSD-95 mutant without palmitoylation sites did not alter any measured NMDA or AMPA property, arguing that the effects of PSD-95 overexpression are specific to its ability to regulate receptor trafficking.

Our data suggest that PSD-95 favours the developmental decrease in functional NMDA receptors containing the NR2B subunit from both synaptic and extrasynaptic receptor populations rather than directly regulating NMDA channel properties. These effects seem specific for the NR2B subunit because the amplitude of NMDA-mEPSCs and whole-cell current density were still reduced upon cotransfection of PSD-95 with flag-tagged NR2B but not NR2A. The decrease in NR2B expression by PSD-95

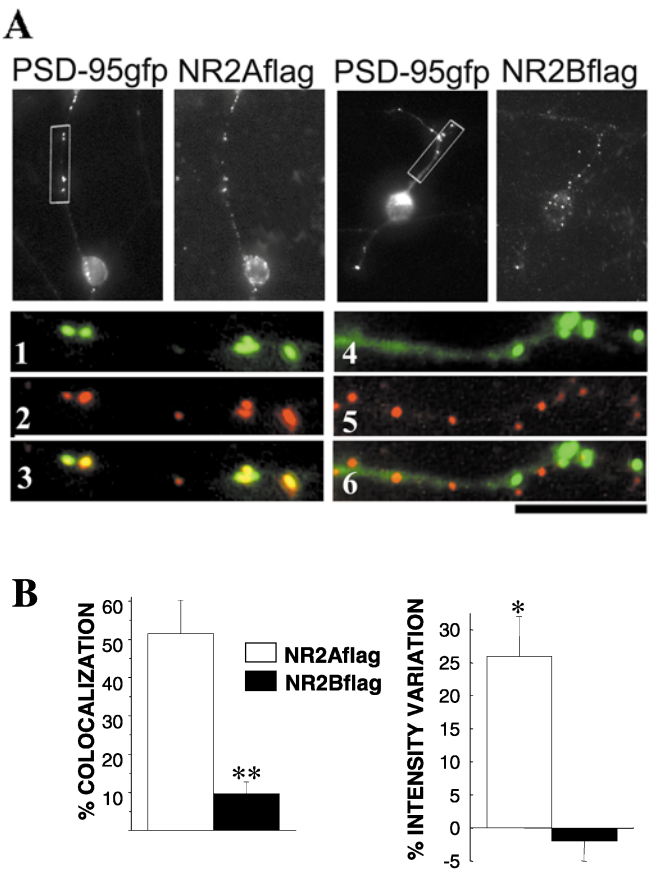

Figure 6. Distinct colocalization of PSD-95gfp with NR2A-flag and NR2B-flag clusters

A, live surface staining of CGCs cotransfected with PSD-95gfp and either NR2A-flag (left) or NR2B-flag (right). Upper panels show PSD-95gfp fluorescence and flag staining. Lower panels (1–6) show a higher magnification of a portion of dendrite (outlined by the box) with PSD-95gfp fluorescence (green, 1 and 4), flag staining (red, 2 and 5) and overlay of PSD-95gfp and flag fluorescence (3 and 6). Calibration bars are 10 μm and 2.5 μm for the insets. *B*, summary of percentage of colocalization of NR2A-flag or NR2B-flag subunit clusters with PSD-95gfp puncta and percentage of intensity variation of colocalizing clusters *vs.* mismatching ones. $n > 15$; * $P < 0.05$,** $P < 0.001$ ANOVA.

would allow the free access of new NR2A subunits (generated either by transfection or by the normal developmental increase in expression) to the synaptic pool. An activity-dependent increase in dendritic PSD-95 that binds NR2A subunit has been observed in mouse superior colliculus neurons (Yoshii *et al.* 2001). This activity-dependent increase did not bind the remaining NR2 subunits in NR2A knock-out mice (Townsend *et al.* 2001), demonstrating the interaction of PSD-95 and NR2A subunit. PSD-95 involvement in synaptic targeting of NR2A subunit in CGCs is supported by our result that transfection of the NR2A subunit together with PSD-95 increases the size of NMDA-mEPSC when compared to control, in contrast to the decrease seen with the transfection of PSD-95 together with the NR2B subunit. Indeed, transfection of flag-tagged NR2 subunits and live surface staining with anti-flag antibody revealed that NR2A, but not NR2B, clusters colocalize better with PSD-95gfp puncta and show higher intensity. The decrease in NMDA-mEPSC duration with PSD-95gfp overexpression can be overcome by cotransfection with NR2B subunit, as the kinetics of NMDA-mEPSCs from PSD-95gfp/NR2B-flag-transfected CGCs were not different from untransfected controls. This together with a limited expression of PSD-95 in immature cerebellar neurons may underlie the differences between our findings and those seen in hippocampal neurons (El-Husseini *et al.* 2002; Schnell *et al.* 2002). The reported lack of action of PSD-95 overexpression on NMDA receptors in hippocampal neurons may be due to a higher expression of PSD-95 in the hippocampus compared to the cerebellum (Fukaya *et al.* 1999; Fukaya & Watanabe, 2000).

Our findings extend to CGCs the proposal of a crucial role for PSD-95 in the maturation of excitatory synapses and suggest a specific role in regulating distinct NMDA receptor subtypes during development in these neurons.

REFERENCES

Cathala L, Misra C & Cull-Candy S (2000). Developmental profile of the changing properties of NMDA receptors at cerebellar mossy fiber-granule cell synapses. *J Neurosci* **20**, 5899–5905.

Chen L, Chetkovich DM, Petralia RS, Sweeney NT, Kawasaki Y, Wenthold RJ, Bredt DS, & Nicoll RA (2000). Stargazing regulates synaptic targeting of AMPA receptors by two distinct mechanisms. *Nature* **408**, 936–943.

Clark BA, Farrant M & Cull-Candy SG (1997). A direct comparison of the single-channel properties of synaptic and extrasynaptic NMDA receptors. *J Neurosci* **17**, 107–116.

Craven SE, El-Husseini AE & Bredt DS. (1999). Synaptic targeting of the postsynaptic density protein PSD-95 mediated by lipid and protein motifs. *Neuron* **22**, 497–509.

Cull-Candy S, Brickley S & Farrant M (2001). NMDA receptor subunits: diversity, development and disease. *Curr Opin Neurobiol* **11**, 327–335.

El-Husseini AE, Schnell E, Chetkovich DM, Nicoll RA & Bredt DS (2000). PSD-95 involvement in maturation of excitatory synapses. *Science* **290**, 1364–1368.

Fukaya M, Ueda H, Yamauchi K, Inoue Y & Watanabe M (1999). Distinct spatiotemporal expression of mRNAs for the PSD-95/SAP90 protein family in the mouse brain. *Neurosci Res* **33**, 111–118.

Fukaya M & Watanabe M (2000). Improved immunohistochemical detection of postsynaptically located PSD-95/SAP90 protein family by protease section pretreatment: a study in the adult mouse brain. *J Comp Neurol* **426**, 572–586.

Gallo V, Kingsbury A, Balazs R & Jorgensen OS (1987). The role of depolarization in the survival and differentiation of cerebellar granule cells in culture. *J Neurosci* **7**, 2203–2213.

Garner CC, Nash J & Huganir RL (2000). PDZ domains in synapse assembly and signaling. *Trends Cell Biol* **10**, 274–280.

Hamori J & Somogyi J (1983). Differentiation of cerebellar mossy fiber synapses in the rat: a quantitative electron microscope study. *J Comp Neurol* **220**, 365–377.

Hawkins LM, Chazot PL & Stephenson FA (1999) Biochemical evidence for the co-association of three *N*-methyl-D-aspartate (NMDA) R2 subunits in recombinant NMDA receptors. *J Biol Chem* **274**, 27211–27218.

Kennedy MB (1998). Signal transduction molecules at the glutamatergic postsynaptic membrane. *Brain Res Brain Res Rev* **26**, 243–257.

Kornau HC, Seeburg PH & Kennedy MB (1997). Interaction of ion channels and receptors with PDZ domain proteins. *Curr Opin Neurobiol* **7**, 368–373.

Losi G, Prybylowski K, Fu Z, Luo JH & Vicini S (2002). Silent synapses in developing cerebellar granule neurons. *J Neurophysiol* **87**, 1263–1270.

McIlhinney RA, Le Bourdelles B, Molnar E, Tricaud N, Streit P & Whiting PJ (1998). Assembly, intracellular targeting, and cell surface expression of the human *N*-methyl-D-aspartate receptor subunits NR1a and NR2A in transfected cells. *Neuropharmacology* **37**, 1355–1367.

Mellor JR, Merlo D, Jones A, Wisden W & Randall AD (1998). Mouse cerebellar granule cell differentiation: electrical activity regulates the $GABA_A$ receptor α6 subunit gene. *J Neurosci* **18**, 2822–2833.

Monyer H, Burnashev H, Laurie DJ, Sakmann B & Seeburg PH (1994). Developmental and regional expression in the rat brain and functional properties of the four NMDA receptors. *Neuron* **12**, 529–540.

Murase K, Ryu PD & Randic M (1989). Excitatory and inhibitory amino acids and peptide-induced responses in acutely isolated rat spinal dorsal horn neurons. *Neurosci Lett* **103**, 56–63.

Palay SL & Chan-Palay V (1974). *Cerebellar Cortex: Cytology and Organization*, pp. 142–179. Springer-Verlag, New York.

Prybylowski K, Fu Z, Losi G, Hawkins LM, Luo J, Chang K, Wenthold RJ & Vicini S (2002). Relationship between availability of NMDA receptor subunits and their expression at the synapse. *J Neurosci* **22**, 8902–8910.

Rumbaugh G & Vicini S (1999). Distinct synaptic and extrasynaptic NMDA receptors in developing cerebellar granule neurons. *J Neurosci* **19**, 1–8.

Schnell E, Sizemore M, Karimzadegan S, Chen L, Bredt DS & Nicoll RA (2002). Direct interactions between PSD-95 and stargazin control synaptic AMPA receptor number. *Proc Natl Acad Sci U S A* **99**, 13902–13907.

Silver RA, Traynelis SF & Cull-Candy SG (1992). Rapid-time-course miniature and evoked excitatory currents at cerebellar synapses in situ. *Nature* **355**, 163–166.

Townsend T, Mishina M & Constantine-Paton M (2001). Visual activity drives developmental redistribution of synaptic NMDA receptors. *Soc Neurosci Abs* **27**, 362.

Vicini S, Wang JF, Li JH, Zhu WJ, Wang YH, Luo JH, Wolfe BB & Grayson DR (1998). Functional and pharmacological differences between recombinant *N*-methyl-D-aspartate receptors. *J Neurophysiol* **79**, 555–566.

Virginio C, Martina M & Cherubini E (1995). Spontaneous GABA-mediated synaptic currents in cerebellar granule cells in culture. *Neuroreport* **6**, 1285–1289.

Williams K (1993). Ifenprodil discriminates subtypes of the *N*-methyl-D-aspartate receptor: selectivity and mechanisms at recombinant heteromeric receptors. *Mol Pharmacol* **44**, 851–859.

Yoshii A, Sheng M & Constantine-Paton M (2001). Rapid activity dependent dendritic localization of synaptic PSD-95 following eye opening in development but not maturity. *Soc Neurosci Abs* **27**, 362.

Ziff EB (1997). Enlightening the postsynaptic density. *Neuron* **19**, 1163–1174.

Acknowledgements

Supported by the Pharmacology Research Associate (PRAT) Program (K.P.), the NIDCD Intramural Program (K.P. and R.J.W.), and grants MH58946 and MH01680 to S.V. We thank Dr L. Chen for helpful advice on culture procedures. We are grateful to Drs David Bredt, Paul Whiting and Anne Stephenson for the gifts of the PSD-95gfp, NR2A-flag and NR2B-flag constructs, respectively.